

## Formation of the Calcium/Poly(3-Hexylthiophene) Interface: Structure and Energetics

Junfa Zhu,<sup>†,‡</sup> Fabian Bebensee,<sup>§</sup> Wolfgang Hieringer,<sup>||</sup> Wei Zhao,<sup>†</sup>  
Jack H. Baricuatro,<sup>‡</sup> Jason A. Farmer,<sup>‡</sup> Yun Bai,<sup>§</sup> Hans-Peter Steinrück,<sup>§</sup>  
J. Michael Gottfried,<sup>\*,§</sup> and Charles T. Campbell<sup>\*,‡</sup>

National Synchrotron Radiation Laboratory, University of Science and Technology of China, Hefei 230029, Peoples Republic of China, Department of Chemistry, University of Washington, Seattle, Washington 98195-1700, and Lehrstuhl für Physikalische Chemie II and Interdisciplinary Center for Molecular Materials, and Lehrstuhl für Theoretische Chemie, Universität Erlangen-Nürnberg, Egerlandstr. 3, 91058 Erlangen, Germany

Received June 21, 2009; E-mail: michael.gottfried@chemie.uni-erlangen.de;  
campbell@chem.washington.edu

**Abstract:** The adsorption of Ca on poly(3-hexylthiophene) (P3HT) has been studied by adsorption microcalorimetry, atomic beam/surface scattering, X-ray photoelectron spectroscopy (XPS), low-energy He<sup>+</sup> ion scattering spectroscopy (LEIS), and first-principles calculations. The sticking probability of Ca on P3HT is initially 0.35 and increases to almost unity by 5 ML. A very high initial heat of adsorption in the first 0.02 ML (625–500 kJ/mol) is attributed to the reaction of Ca with defect sites or residual contamination. Between 0.1 and 0.5 ML, there is a high and nearly constant heat of adsorption of 405 kJ/mol, which we ascribe to Ca reacting with subsurface sulfur atoms from the thiophene rings of the polymer. This is supported by the absence of LEIS signal for Ca and the shift of the S 2p XPS binding energy by –2.8 eV for reacted S atoms. The heat of adsorption decreases above 0.6 ML coverage, reaching the sublimation enthalpy of Ca, 178 kJ/mol, by 4 ML. This is attributed to the formation of Ca nanoparticles and eventually a continuous solid Ca film, on top of the polymer. LEIS and XPS measurements, which show only a slow increase of the signals related to solid Ca, support this model. Incoming Ca atoms are subject to a kinetic competition between diffusing into the polymer to react with subsurface thiophene units versus forming or adding to three-dimensional Ca clusters on the surface. At ~1.6 ML Ca coverage, Ca atoms have similar probabilities for either process, with the former dominating at lower coverage. Ultimately about 1.6 ML of Ca (1.2 × 10<sup>15</sup> atoms/cm<sup>2</sup>) reacts with S atoms, corresponding to a reacted depth of ~3 nm, or nearly five monomer-unit layers. Density-functional theory calculations confirm that the heat of reaction and the shift of the S 2p signal are consistent with Ca abstracting S from the thiophene rings to form small CaS clusters.

### 1. Introduction

Interfaces between metals and semiconducting,  $\pi$ -conjugated polymers (such as derivatives of poly(phenylenevinylene), polyfluorene, and polythiophene) play an important role in organic electronic and optoelectronic devices, such as organic light-emitting diodes (OLEDs),<sup>1</sup> photovoltaic cells,<sup>2</sup> photodiodes, and field effect transistors.<sup>3–5</sup> One of the best electrode/polymer combinations in terms of performance in solar cell applications is Ca on regioregular poly(3-hexylthiophene) (rr-

P3HT), which is usually employed with an Al film added on top of the Ca film as a protective coating.<sup>6–10</sup> Here we study the structure and bonding energetics of Ca/rr-P3HT interfaces, formed just as they are for device applications, by depositing Ca onto vacuum-outgassed rr-P3HT films. By simultaneously measuring the heat of adsorption and the sticking probability of the metal atoms as a detailed function of metal coverage, we obtain the first interfacial bonding energies for Ca on P3HT. We also clarify the structural details of this interface and the morphology of the evolving Ca film using high-resolution X-ray photoelectron spectroscopy (XPS) and low-energy He<sup>+</sup> ion

<sup>†</sup> University of Science and Technology of China.

<sup>‡</sup> University of Washington.

<sup>§</sup> Lehrstuhl für Physikalische Chemie II and Interdisciplinary Center for Molecular Materials, Universität Erlangen-Nürnberg.

<sup>||</sup> Lehrstuhl für Theoretische Chemie, Universität Erlangen-Nürnberg.

- (1) Friend, R. H.; Gymer, R. W.; Holmes, A. B.; Burroughes, J. H.; Marks, R. N.; Taliani, C.; Bradley, D. D. C.; Dos Santos, D. A.; Bredas, J. L.; Logdlund, M.; Salaneck, W. R. *Nature* **1999**, *397* (6715), 121–128.
- (2) Coakley, K. M.; McGehee, M. D. *Chem. Mater.* **2004**, *16*, 4533–4542.
- (3) Garnier, F.; Hajlaoui, R.; Yassar, A.; Srivastava, P. *Science* **1994**, *265* (5179), 1684–1686.
- (4) Fahlman, W.; Salaneck, W. R. *Surf. Sci.* **2002**, *500* (1–3), 904–922.
- (5) Salaneck, W. R.; Logdlund, M.; Fahlman, M.; Greczynski, G.; Kugler, T. *Mater. Sci. Eng. Res.* **2001**, *34* (3), 121–146.

(6) Reese, M. O.; White, M. S.; Rumbles, G.; Ginley, D. S.; Shaheen, S. E. *Appl. Phys. Lett.* **2008**, *92*, 053307.

(7) Reese, M. O.; Morfa, A. J.; White, M. S.; Kopidakis, N.; Shaheen, S. E.; Rumbles, G.; Ginley, D. S. *Sol. Energy Mater. Sol. Cells* **2008**, *92*, 746–752.

(8) Paci, B.; Generosi, A.; Albertini, V. R.; Perfetti, P.; de Bettignies, R.; Sentein, C. *Chem. Phys. Lett.* **2008**, *461*, 77–81.

(9) Hsieh, S.-N.; Kuo, T.-Y.; Chong, L.-W.; Wen, T.-C.; Yang, F.-S.; Guo, T.-F.; Chung, C.-T. *IEEE Photon. Tech. Lett.* **2009**, *21*, 109–111.

(10) Bröms, P.; Birgersson, J.; Johansson, N.; Lögdlund, M.; Salaneck, W. R. *Synth. Met.* **1995**, *74*, 179–181.

scattering spectroscopy (LEIS). These results are interpreted with the help of density functional theory (DFT) and MP2 calculations. They reveal a complex interface that involves diffusion of Ca into the polymer coupled with a highly exothermic reaction with the thiophene S atoms, in kinetic competition with Ca particle nucleation and film growth on top of the polymer.

To our knowledge, no other studies exist that probe this Ca/P3HT interface using XPS, LEIS, or adsorption calorimetry. The interactions of vapor-deposited Na, Cu, Ag, Au, Cr, V, and Ti with P3HT have been studied by XPS,<sup>11–13</sup> where the XPS results implied that Na and Cu atoms react exclusively with the S atoms of the P3HT while Cr, V, and Ti react with both the S atom and C atoms of the thiophene ring. Little or no reaction of Ag and Au with P3HT was found. The present results also bring new insight into these previous studies of the adsorption of other metals on P3HT.

By calorimetrically measuring the strength of bonding between metal and the polymer here, these results provide direct insight into the mechanical stability of the interface and indirect insight into interfacial electronic properties such as the interfacial dipoles and band offset. Coupled with our high-resolution XPS measurements, this provides even more powerful understanding of these electronic details. Metal–polymer interfacial bond energies have only recently been measured and only for very few systems.<sup>14–17</sup> The present results thus also provide thermodynamic information of general interest to a broad range of metal/polymer systems.

## 2. Experimental and Computational Details

The P3HT used for these studies was regioregular poly(3-hexylthiophene) (rr-P3HT, see inset in Figure 1a), with >98% head-to-tail addition and MW  $\approx$  30 000 amu. It was obtained from Sigma-Aldrich and purified via Soxhlet extraction as in ref 18. The bulk material was purified by extraction with methanol and then acetone. The fraction used in this study was collected from a final extraction with  $\text{CHCl}_3$  and used as is. For calorimetric, sticking probability, and LEIS measurements, the P3HT thin films were prepared by directly spin-coating a P3HT solution in chloroform (0.3 wt %) onto a pyroelectric heat detector sheet with 1000 rpm for 10 s, followed by 2000 rpm for 30 s in dry nitrogen atmosphere. In order to obtain a bulklike polymer thin film, this sequence was performed twice on each sample with 60  $\mu\text{L}$  of solution dispensed in each run. In this way, it was ensured that the film thickness was  $\sim$ 100 nm, as estimated with atomic force microscopy (AFM) by scratching away some of the film using the AFM tip and then looking at the step height. To avoid photodegradation of the polymer, the samples were shielded from light and transferred into vacuum as quickly as possible. The morphology of these thin P3HT films, as monitored by AFM, was flat and homogeneous; the surface roughness (root-mean-square, rms) equaled  $0.4 \pm 0.2$  nm on a  $2 \times 2 \mu\text{m}^2$  area. Before measurements, the P3HT samples were placed in ultrahigh vacuum and subsequently evacuated to below  $3 \times 10^{-8}$  mbar and heated for 8 h to 60  $^\circ\text{C}$ , just below the polymer's glass

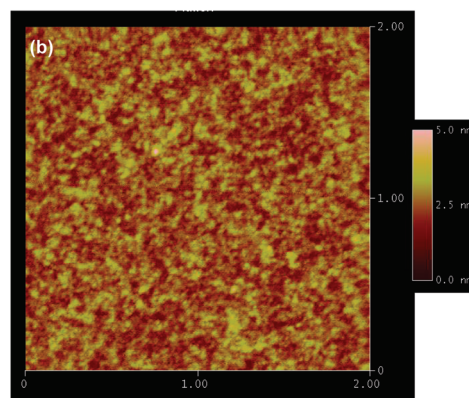
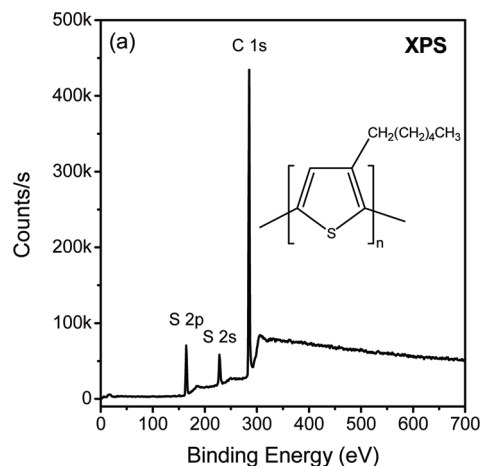


**Figure 1.** (a) Survey XP spectrum ( $h\nu = 1486.6$  eV) and (b) AFM micrograph ( $2 \mu\text{m} \times 2 \mu\text{m}$ ) of a clean rr-P3HT film. Analysis of the AFM results indicate a film thickness of  $\sim$ 100 nm and a surface roughness (rms) of  $\sim$ 0.4 nm. The color-coded height scale extends from 0 to 5 nm. The molecular structure of poly(3-hexylthiophene) is shown in the inset in part a.

transition temperature of 65  $^\circ\text{C}$ ,<sup>19</sup> to remove any residual solvent and surface contaminants. Survey XP spectra of such P3HT films (see Figure 1a for a representative example) did not show any Cl signal, indicating that this treatment is sufficient to remove the chloroform solvent. A representative AFM image of a typical freshly spin-coated P3HT film is shown in Figure 1b.

The experiments were performed in three separate ultrahigh vacuum (UHV) systems. The microcalorimetric methods for measuring the adsorption energies of metals on polymer surfaces have been described in detail previously.<sup>16</sup> Briefly, the adsorption microcalorimeter is housed in a UHV chamber with a base pressure of  $2 \times 10^{-10}$  mbar, which is equipped with a hemispherical electron energy analyzer (Leybold-Heraeus EA 11/100) for Auger electron spectroscopy (AES) and LEIS, a UTI quadrupole mass spectrometer (QMS), an ion gun (Leybold-Heraeus IQE 12/38), and a quartz crystal microbalance (QCM). This analysis chamber and the pulsed metal atomic beam used in this study are the same as those described elsewhere.<sup>20</sup> A sample preparation chamber (base pressure of  $8 \times 10^{-9}$  mbar) in which multiple samples can be stored, outgassed, and transferred into the analysis chamber is attached to the analysis chamber.<sup>16</sup> The heat detector of the calorimeter is a 9  $\mu\text{m}$  thick sheet of highly sensitive pyroelectric  $\beta$ -polyvinylidene fluoride (PVDF) coated on both sides with aluminum (Measurement Specialties, Inc.).

- (11) Mikalo, R. P.; Schmeisser, D. *Synth. Met.* **2002**, *127*, 273–277.
- (12) Lachkar, A.; Selmani, A.; Sacher, E.; Leclerc, M.; Mokhliss, R. *Synth. Met.* **1994**, *66*, 209–215.
- (13) Lachkar, A.; Selmani, A.; Sacher, E. *Synth. Met.* **1995**, *72*, 73–80.
- (14) Murdey, R.; Stuckless, J. T. *J. Am. Chem. Soc.* **2003**, *125*, 3995–3998.
- (15) Hon, S. S.; Richter, J.; Stuckless, J. T. *Chem. Phys. Lett.* **2004**, *385*, 92–95.
- (16) Diaz, S. F.; Zhu, J. F.; Harris, J. J. W.; Goetsch, P.; Merte, L. R.; Campbell, C. T. *Surf. Sci.* **2005**, *598*, 22–34.
- (17) Zhu, J. F.; Goetsch, P.; Ruzycski, N.; Campbell, C. T. *J. Am. Chem. Soc.* **2007**, *129*, 6432–6441.
- (18) Bartholomew, G. P.; Heeger, A. J. *Adv. Funct. Mater.* **2005**, *15*, 677–682.

- (19) Yang, H.; Shin, T. J.; Bao, Z.; Ryu, C. Y. *J. Polym. Sci., Polym. Phys.* **2007**, *45*, 1303–1312.
- (20) Stuckless, J. T.; Frei, N. A.; Campbell, C. T. *Rev. Sci. Instrum.* **1998**, *69*, 2427–2438.

For calorimetry, freshly spin-coated P3HT on such a detector sheet was mounted on a specially designed sample platen (see ref 16) and placed on the platen carriage in the sample preparation chamber, which was subsequently evacuated to below  $3 \times 10^{-8}$  mbar and heated as described above. The reflectivity of each such sample at the He–Ne laser wavelength (632.8 nm) was measured ex situ using an integrating sphere and found to vary around  $0.7 \pm 0.1$ . The accuracy of the reflectivity measurement for an individual sample had a much lower uncertainty of  $\pm 2\%$ . More calorimetry details regarding polymer sample preparation, sample platen, and multiple sample carriage can be found in ref 16.

The pulsed Ca atom beam source has been described in detail previously.<sup>17,20</sup> Briefly, it is generated from an effusive vapor source and chopped into 100 ms long pulses with a repetition rate of 0.5 Hz. The beam is collimated to provide a 4 mm diameter deposition area on the polymer surface. The typical oven operating temperature was  $\sim 1000$  K, resulting in typically 0.007 ML of Ca in each metal pulse. The pulse-to-pulse variation in the Ca dose per pulse was  $< 2\%$  in a given experimental run. Here, the Ca coverage  $\theta_{\text{Ca}}$  (in ML) is defined as the number of Ca atoms per area in a close-packed layer (111) of Ca atoms with lattice parameters of bulk Ca (1 ML =  $7.4 \times 10^{14}$  atoms/cm<sup>2</sup>). The part of the heat signal caused by thermal radiation from the hot oven was determined using a BaF<sub>2</sub> window, transmitting a known fraction of the radiation (95%, measured before and after each experiment), to block the metal beam, so that no metal atoms could impinge onto the P3HT surface. This oven radiation (0.07  $\mu\text{J}/\text{pulse}$ , or  $72.8 \pm 0.4$  kJ of absorbed radiation per mole of dosed Ca) is subtracted from the total measured signal. Small changes of sample reflectivity due to Ca adsorption were determined by measuring the variation in detector response to heat input from a fixed energy He–Ne laser as a function of coverage, from which the relative changes in absorbency (reflectivity) as a function of Ca coverage were extracted (see the Supporting Information for further details).

The Ca flux was measured with a calibrated QCM, which is placed in a position identical to the position of the sample during heat measurements. The sticking probability is measured by a modified King–Wells method, using a quadrupole mass spectrometer (QMS) mounted in line-of-sight to the sample at the “magic angle” of 35° from the surface normal<sup>21</sup> to detect the nonsticking fraction of metal atoms. The mass spectrometer signal is calibrated to a so-called “zero-sticking” reference signal, which is provided by measuring the integrated desorption of a known amount of multilayer Ca from a Ta foil, located at the same position as the sample, corrected for average velocity.<sup>17,20,22</sup> In order to avoid damage of the P3HT sample surface by electrons emitted from the ion source of the mass spectrometer during the measurements, a metal mesh with a bias voltage of  $-500$  V was placed between the sample and the mass spectrometer.

To convert the measured internal energy changes into standard enthalpy changes at the sample temperature (300 K), the excess translational energy of the metal gas atoms at the oven temperature, above that for a 300 K Maxwell–Boltzmann distribution (0.05  $\mu\text{J}/\text{pulse}$ ), is subtracted, and a small pressure–volume work term ( $RT$ ) is added, as described elsewhere.<sup>17,20</sup> In the high-coverage regime, where a bulklike film has formed, this corrected standard enthalpy of adsorption is thus directly comparable to the standard heat of sublimation of the metal. The measured heats can be expressed as the enthalpy of adsorption per mole adsorbed metal by dividing the absolute heats by the amount of adsorbed Ca in each pulse.

Ion scattering spectroscopy (LEIS) was performed to monitor the growth mode of Ca atoms on the P3HT surface. All LEIS experiments were carried out using <sup>4</sup>He<sup>+</sup> ions with 1 keV primary energy using a focused ion gun (Leybold-Heraeus IQE 12/38). Typical ion fluxes were  $\sim 100$  nA/cm<sup>2</sup> and total ion dosages per experiment  $\sim 6$   $\mu\text{C}/\text{cm}^2$ .

For the XPS measurements, the P3HT thin films were prepared by spin-coating the P3HT in chloroform solution onto Si wafer substrates or, alternatively, 0.1 mm thick Al foil using the same preparation as described above. The XPS investigations at higher photon energy (1486.6 eV) were performed with a commercial X-ray photoelectron spectrometer (Scienta ESCA-200) equipped with an Al K $\alpha$  X-ray source with monochromator and a hemispherical energy analyzer (SES-200). The overall energy resolution of the spectrometer was 0.3 eV. The UHV system (base pressure below  $2 \times 10^{-10}$  mbar) also comprises a mass spectrometer (Pfeiffer HiQuad QMA 400), various evaporators, and a sample load-lock system. The reported XPS binding energies are referenced to the Fermi edge of a clean Ag(111) surface ( $E_{\text{B}} \equiv 0$ ). The XP spectra were recorded in normal emission. Ca was evaporated with a home-built Knudsen cell evaporator at a temperature of 873 K, measured at the quartz glass crucible. The resulting flux, typically 2  $\text{Å}/\text{min}$  at the sample position, was measured by monitoring the attenuation of the substrate signals upon deposition of the Ca onto an Au foil.

The XPS measurements at lower photon energy (200 eV) were carried out in the Surface Physics Endstation at beamline U18 in the National Synchrotron Radiation Laboratory (NSRL) in Hefei, China. This beamline is connected to a bending magnet and equipped with three gratings that cover photon energies from 10 to 250 eV with a resolving power ( $E/\Delta E$ ) better than 1000. The endstation consists of three UHV chambers—analysis chamber, sample preparation chamber, and molecular beam epitaxy (MBE) chamber—the base pressures of which are  $3 \times 10^{-11}$ ,  $5 \times 10^{-10}$  and  $2 \times 10^{-10}$  mbar, respectively, and a sample load-lock system. The analysis chamber is equipped with a VG ARUPS10 angle-resolved photoelectron spectrometer and a twin anode X-ray source. The sample preparation chamber comprises a small electron energy analyzer, a cold cathode ion source, and an electron gun. The MBE chamber houses an electron gun for reflection high energy electron diffraction (RHEED), various Knudsen cell evaporators, and a QCM for monitoring deposition rates. Each freshly spin-coated P3HT sample was introduced into the sample preparation chamber first and then transferred into the MBE chamber. Before Ca deposition, the P3HT samples were treated in the same way as those for calorimetric measurements. Ca deposition was performed with a similar rate as that for LEIS measurements,  $\sim 3$   $\text{Å}/\text{min}$ .

To estimate reaction enthalpies and XPS core level shifts involving calcium sulfide clusters, molecular and periodic DFT calculations on Ca<sub>n</sub>S<sub>n</sub> clusters of various size ( $n = 1, 4, 32, 108$ ) and on solid (CaS)<sub>∞</sub> (rock-salt structure type) have been performed using the PBE<sup>23</sup> functional. The finite clusters have been optimized within  $T_d$  point group symmetry with a basis set of polarized double- $\zeta$  quality (SV(P)) using the Turbomole<sup>24–26</sup> program. Initial-state core level shifts have been estimated from the computed orbital energies for these clusters and thiophene. The periodic calculations have been performed using the program VASP (Vienna ab initio simulation program).<sup>27–30</sup> Both cell and basis have been optimized using  $21 \times 21 \times 21$   $k$ -points (Monkhorst–Pack) and a plane-wave energy cutoff of 350 eV. The interaction energy of a Ca atom with a thiophene molecule has been calculated at the MP2/TZVPP<sup>31,32</sup>

(21) Pauls, S. W.; Campbell, C. T. *Surf. Sci.* **1990**, *226*, 250–256.

(22) Zhu, J.; Farmer, J. A.; Ruzycski, N.; Xu, L.; Campbell, C. T.; Henkelman, G. *J. Am. Chem. Soc.* **2008**, *130*, 2314–2322.

(23) Perdew, J. P.; Burke, K.; Ernzerhof, M. *Phys. Rev. Lett.* **1996**, *77*, 3865–3868. Perdew, J. P.; Burke, K.; Ernzerhof, M. *Phys. Rev. Lett.* **1997**, *78*, 1396.

(24) Ahlrichs, R., et al. *TURBOMOLE*, version 5.9; University of Karlsruhe.

(25) Ahlrichs, R.; Bar, M.; Häser, M.; Horn, H.; Kölmel, C. *Chem. Phys. Lett.* **1989**, *162*, 165–169.

(26) Eichkorn, K.; Treutler, O.; Öhm, H.; Häser, M.; Ahlrichs, R. *Chem. Phys. Lett.* **1995**, *242*, 652–660.

(27) VASP, Version 4.6; Institut für Materialphysik, Universität Wien.

(28) Kresse, G.; Hafner, J. *Phys. Rev. B* **1993**, *48*, 13115–13118.

(29) Kresse, G.; Furthmüller, J. *Phys. Rev. B* **1996**, *54*, 11169–11186.

(30) Kresse, G.; Furthmüller, J. *Comput. Mater. Sci.* **1996**, *6*, 15–50.

(31) Weigend, F.; Häser, M. *Theor. Chem. Acc.* **1997**, *97*, 331–340.

(32) Weigend, F.; Häser, M.; Patzelt, H.; Ahlrichs, R. *Chem. Phys. Lett.* **1998**, *294*, 143–152.

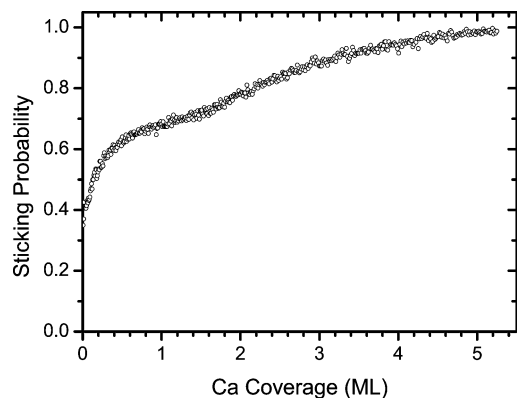


**Figure 2.** Sticking probability of Ca on a P3HT film at 300 K plotted as a function of Ca coverage. Monolayer coverage (1 ML) is defined as  $7.4 \times 10^{14}$  Ca atoms per  $\text{cm}^2$  [the Ca(111) packing density].

level using the Turbomole program. To that end, the geometries of a Ca–thiophene complex have been optimized at the same level of theory.

### 3. Results

**3.1. Sticking Probability.** In order to determine the amount of Ca that actually adsorbs on the P3HT surface and causes the heats of adsorption and reaction measured by microcalorimetry, the sticking probability of Ca on P3HT must be known. Figure 2 shows the sticking probability as a function of Ca coverage at 300 K. The curve is the average of three independent, yet highly reproducible, experiments. Three distinct regimes can be identified. In the low coverage regime, the sticking probability increases rapidly from an initial value of 0.35 to 0.6 at a coverage of 0.5 ML. In the range of intermediate coverages between 0.5 and 1.5 ML, the curve is less steep and a sticking probability of 0.7 is reached at 1.5 ML. Above 1.5 ML, the sticking probability further increases with a steeper slope until it asymptotically approaches unity around 5 ML. Note that all coverages reported in this paper refer to the amount of Ca that is actually adsorbed on the surface. These coverages are calculated by multiplying the Ca dosage—the flux of the atomic beam multiplied by the deposition time—by the sticking probability integrated over the total dosage.

**3.2. Low-Energy Ion Scattering (LEIS).** Metal films growing on polymer surfaces form a variety of structures, including three-dimensional (3D) particles and continuous films. In addition, diffusion of the metal atoms to the subsurface region and reaction with functional groups of the polymer have been observed.<sup>17,33–36</sup> Knowledge of the growth mode is, therefore, an essential prerequisite for interpreting the measured coverage-dependent heats of adsorption.

LEIS with  $\text{He}^+$  ions provides a valuable tool for the evaluation of the growth mode of Ca on P3HT, because it is element-specific and extremely surface-sensitive, that is, it probes only the topmost atomic layer. Figure 3 shows the evolution of the normalized LEIS peak intensity of Ca as a function of Ca coverage with the inset displaying the low coverage regime in

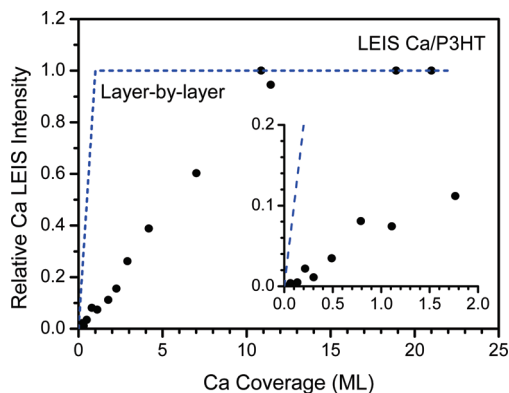


**Figure 3.** The relative integrated Ca LEIS peak intensity as a function of Ca coverage on P3HT at a sample temperature of 300 K, with all intensities normalized with respect to the saturation signal obtained for high Ca coverages. The blue dashed line indicates the expected trace for layer-by-layer growth. The inset shows a blowup of the low-coverage region.

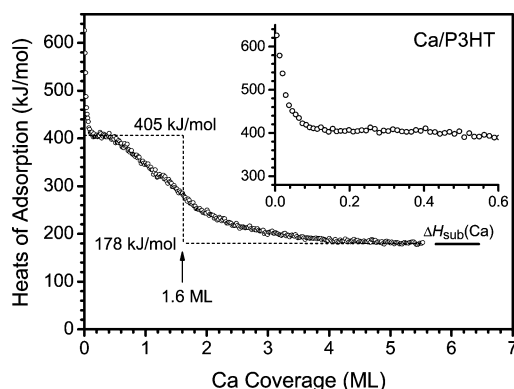


**Figure 4.** The differential heat of adsorption of Ca atoms on a rr-P3HT surface as a function of Ca coverage at 300 K. The inset shows an enlarged plot of the low-coverage range. The dashed line refers to a two-site model for Ca adsorption that is explained in the text. On the right-hand side, the sublimation enthalpy of Ca,  $\Delta H_{\text{sub}}(\text{Ca}) = 178$  kJ/mol, is displayed.

more detail. We proved that ion beam damage was not influencing this curve by repeating measurements at several Ca coverages with  $\sim 3$ -fold less ion exposure and saw no differences. The data reveal that the intensity of the Ca signal increases linearly until saturation is reached around 11 ML. For comparison, a dashed line representing the layer-by-layer growth mode is displayed. The much slower growth of the observed Ca peak intensity is consistent with 3D island growth, resulting in tall, large Ca islands, which eventually coalesce into a continuous film around 11 ML, combined with diffusion of Ca atoms into the subsurface region of the polymer film at low Ca coverages. (Since this curve would have the same qualitative behavior with or without this added subsurface diffusion, the LEIS data alone does not prove subsurface diffusion.)

**3.3. Heats of Adsorption.** Figure 4 presents the differential heat of adsorption of Ca on P3HT averaged over three experimental runs at 300 K as a function of coverage. These measured heats represent the standard enthalpies at 300 K. The inset shows the low-coverage region (0–0.6 ML) in more detail. The pulse-to-pulse standard deviation of the heats of adsorption at high coverages, where the heat is independent of coverage, is less than 2 kJ/mol for a pulse size of approximately 0.01 ML.

As can be seen, the heat of adsorption drops very quickly from an initial value of 625 to  $\sim 405$  kJ/mol, where it remains almost unchanged in the coverage range 0.1–0.6 ML. Beyond 0.6 ML, the heat of adsorption starts to decrease and, above 4

- (33) Bebin, P.; Prud'Homme, R. E. *Chem. Mater.* **2003**, *15*, 965.  
 (34) Strunskus, T.; Zaporozhchenko, V.; Behnke, K.; von Bechtolsheim, C.; Faupel, F. *Adv. Eng. Mater.* **2000**, *2*, 489–492.  
 (35) Smithson, R. L. W.; McClure, D. J.; Evans, D. F. *Thin Solid Films* **1997**, *307*, 110–112.  
 (36) Zaporozhchenko, V.; Zekonyte, J.; Biswas, A.; Faupel, F. *Surf. Sci.* **2003**, *532*, 300–305.

ML, asymptotically approaches the absolute value of the reported bulk heat of Ca sublimation ( $\Delta H_{\text{sub}} = 178 \text{ kJ/mol}$ )<sup>37</sup> to within 2 kJ/mol. This agreement confirms the absolute accuracy of our heat and flux calibrations.

The sharp decrease in the heat of adsorption occurring at very low coverages (0–0.05 ML) is indicative of a small concentration of adsorption sites on the P3HT surface (or in the near-subsurface) that bind Ca very strongly. These sites may originate from impurities, such as residual chloroform or adsorbed water, or intrinsic surface defects. On the basis of the calorimetry data, the number of such sites is very low (<0.05 ML), which is consistent with the fact that they were not detected by XPS. This implies that Ca initially populates some very weakly bound, transient adsorption state (precursor),<sup>38</sup> which can rapidly diffuse across and possibly into the polymer subsurface and desorb again if it does not find a stronger binding site or if the reaction with this binding site is not successful because of an activation barrier. Such a weakly bound transient species is expected, since the interaction of Ca with the dominant  $\text{CH}_2$ ,  $\text{CH}$ , and  $\text{CH}_3$  groups of the polymer (these groups are most probably exposed on the surface to minimize the surface energy<sup>39</sup>) is only a very weak attraction.

After these few sites are saturated, Ca adsorbing on P3HT releases a heat of adsorption of about 405 kJ/mol. This suggests a strong interaction between Ca and some site on or below the polymer surface, as this heat is much higher than that of Ca adsorbed on Ca (178 kJ/mol). From the appearance and growth of a strongly shifted S 2p XPS peak (see below) that correlates in coverage with this high heat, we conclude that weakly adsorbed Ca diffuses to the subsurface and preferentially binds to the sulfur atoms in the thiophene rings. Thus, the relatively high heat of adsorption at low and medium coverages reflects the chemical interaction between Ca and the S atoms. Above 4 ML, the curve reaches the heat of sublimation of Ca, indicating that adsorbing Ca atoms are added to large, bulklike 3D Ca particles. The smooth decrease of the heat of adsorption between 1 and 4 ML indicates that both processes occur simultaneously and that the formation of 3D Ca clusters becomes predominant as the coverage increases.

**3.4. X-ray Photoelectron Spectroscopy (XPS).** Figure 5a shows high-resolution XP spectra of the S 2p region for various coverages of Ca on P3HT. The spectra were recorded using synchrotron radiation with a photon energy of 200 eV. The spin–orbit splitting of the S 2p peak is well-resolved with a spacing of 1.2 eV; the respective binding energies (165.0 and 166.2 eV) agree well with previous experimental results.<sup>12,13</sup> Upon Ca deposition, two significant changes can be observed in the spectra: (a) damping of the original S 2p signal of pristine (“unreacted”) P3HT and (b) the appearance of a new doublet shifted by 2.8 eV toward lower BE relative to the original S 2p signal. The signal of pristine P3HT disappears for Ca coverages above 1.3 ML, while the new feature (of “reacted” P3HT) can still be detected, albeit with very low intensity, at the maximum coverage reached in this experiment (6 ML).

For comparison, the results of a similar experiment using a monochromatized Al  $K\alpha$  source ( $h\nu = 1486.6 \text{ eV}$ ) are shown in Figure 5b. Here, the kinetic energy ( $E_{\text{kin}}$ ) of the S 2p

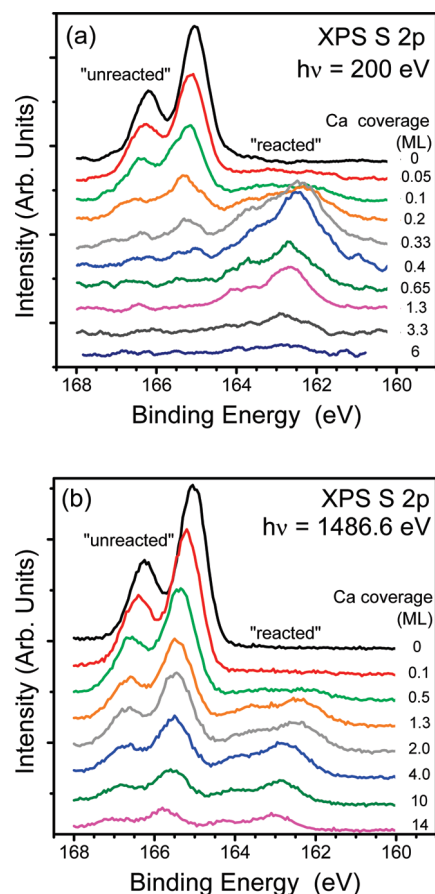


**Figure 5.** XP spectra of the S 2p region for different Ca coverages on P3HT recorded with photon energies of (a) 200.0 eV<sup>53</sup> and (b) 1486.6 eV.

photoelectrons and, consequently, their inelastic mean free path (IMFP) are significantly higher than in the above experiments with 200 eV photons. As a result of the thus increased probe depth, the original S 2p signal of pristine P3HT is visible for all Ca coverages up to 14 ML. The different attenuation lengths for electrons in the two experiments provide information on the diffusion of Ca into the polymer, as will be discussed in section 4. With increasing Ca coverage, the positions of the S 2p signals shift considerably (up to around 0.5 eV at 10 ML coverage) toward higher binding energies. Since the same shifts are observed in the C 1s peaks (Figure 6), they are most likely due to downward band bending (mainly during the first ML of Ca deposition) associated with long-range electron donation into the polymer.<sup>40</sup> Beyond this band bending, the C 1s signal is much less affected by the deposition of Ca than the S 2p signal, indicating that Ca predominantly reacts with the sulfur rather than with the carbon-containing backbone of the polymer or its side chains. The Ca 2p signal (not shown) initially appears at a binding energy of 348.1 eV. With increasing Ca coverage, a shoulder arises on the low binding energy side, which grows into a peak located at 347.1 eV due to 3D solid Ca (at 14 ML). Thus, the Ca 2p signal of “reacted” Ca (that is, Ca that chemically reacts with the polymer) is shifted by +1.0 eV toward higher binding energy relative to the signal of pure Ca multilayers. (After correction for band bending, the shift is even higher, +1.5 eV.)

(37) Lide, D. R. *CRC Handbook of Chemistry and Physics*, 87th ed.; CRC Press: Boca Raton, FL, 2006.

(38) Kisliuk, P. J. *Phys. Chem. Solids* **1957**, *3*, 95–101.

(39) Gregonis, D. E.; Andrade, J. D. In *Surface and Interfacial Aspects of Biomedical Polymers, Surface Chemistry and Physics*; Andrade, J. D., Ed.; Plenum: New York, 1985.

(40) Ettetgui, E.; Hsieh, B. R.; Gao, Y. *Polym. Adv. Technol.* **1997**, *8*, 408–416.

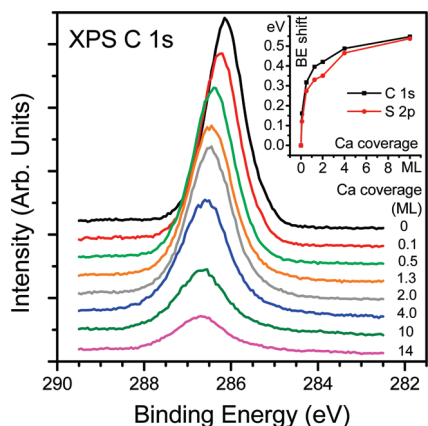


**Figure 6.** C 1s XP spectra of Ca adsorption on P3HT, recorded with a photon energy of 1486.6 eV. Inset: Binding energy shift as a function of Ca coverage for the S 2p (Figure 5b) and C 1s signals.

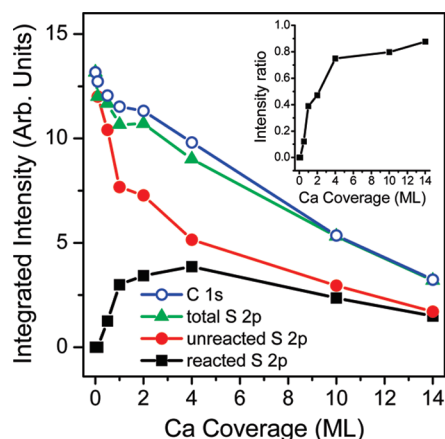


**Figure 7.** Normalized integrated intensities for the S 2p (Figure 5b) and C 1s (Figure 6) signals as a function of coverage. For S 2p, the intensities of the components for reacted and unreacted sulfur are displayed separately. Inset: ratio of the S 2p intensities of reacted and unreacted sulfur.

The changes of the C 1s and the S 2p peak intensities as a function of Ca coverage are plotted in Figure 7 for the spectra taken at 1486.6 eV. The figure also shows the separate intensities of the “reacted” and “unreacted” S 2p peaks, as well as their ratio (inset). The intensity of reacted S increases up to 4 ML Ca, above which its intensity decreases due to Ca film growth on top. The reacted:unreacted ratio increases steeply up to a value of 0.75 at 4 ML Ca, after which the curve slowly approaches a saturation value near unity.

To ensure that these XPS relative intensities and line shapes did not change significantly due to X-ray beam damage, XPS spectra of the polymer (before Ca deposition and at some fixed Ca coverages) were taken with greatly decreased and greatly increased beam exposure times, with no significant changes besides the expected signal:noise differences.

#### 4. Discussion

The experimental results from section 3 can be summarized as follows:

- The heat of Ca adsorption on P3HT for low and medium Ca coverages (<4 ML) is very high (~405 kJ/mol) and much larger than the negative heat of Ca sublimation.
- The LEIS intensity of Ca increases 10 times more slowly with Ca coverage than expected for layer-by-layer growth.

- Ca adsorption causes the appearance and growth of a new S 2p XPS peak, which is shifted by 2.8 eV compared to the unreacted portions of the polymer and correlates with the high (~405 kJ/mol) heat of adsorption, whereas the C 1s signal is much less affected.

In the following, we will derive a consistent model of the chemical state of the Ca/P3HT interface from these observations and provide additional support for this model using DFT calculations.

**4.1. Growth Model of Ca on P3HT.** The LEIS data in Figure 4 show that the Ca signal increases much more slowly with Ca coverage than expected for the formation of a continuous first layer and subsequent layer-by-layer and/or three-dimensional (3D) growth. Rather, the data are consistent with 3D growth from the beginning or with diffusion of parts of the adsorbed Ca to the subsurface or bulk region of the polymer. In the first case, the heat of adsorption should approximately equal the negative heat of Ca sublimation, 178 kJ/mol (or less in the case of small clusters, due to the Kelvin effect<sup>41</sup>). However, the measured heats of adsorption (Figure 4) are considerably higher than that for all coverages below 4 ML. Thus, the initial growth must follow the second scenario, that is, diffusion of parts of the adsorbed Ca to the subsurface or bulk region of the polymer (see below for an estimate of the diffusion depth), where a more exothermic reaction takes place than formation of Ca(s). The decrease in the heat of adsorption between 1 and 4 ML shows that a growing amount of the adsorbed Ca contributes to the growth of 3D Ca clusters on the surface and that beyond 4 ML cluster growth is the dominating process. The LEIS data in Figure 4 show that these clusters coalesce around 11 ML, forming a continuous Ca(s) multilayer film on the surface of the polymer.

**4.2. Chemical Reaction between Ca and P3HT.** The high heat of adsorption values at coverages below 4 ML (Figure 4) and the corresponding large S 2p core level shifts of -2.8 eV (Figure 5) indicate that there is a strong chemical interaction between Ca and P3HT. It is unlikely that such a large shift could be caused by a simple bonding mechanism whereby the Ca atom interacts with the S atom in the thiophene ring without breaking its S-C bonds. In addition, our first-principles calculations of a Ca atom interacting with a thiophene molecule in the gas phase show that such an interaction leads to a bond energy of only 17.5 kJ/mol of Ca (MP2 level), which is not nearly as large as the experimental heat of 405 kJ/mol below 0.5 ML. Several such interactions cannot combine on one Ca atom to increase this heat to anywhere near 405 kJ/mol. For this reason, we rule out all interactions that do not involve bond cleavage in the polymer, combined with their replacement by stronger bonds, to explain the observed heat of 405 kJ/mol.

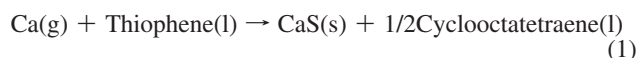
Therefore, it is suggested that a strongly exothermic chemical reaction is taking place that involves bond cleavage and formation. The strongly shifted S 2p peak indicates that this bond cleavage must be at the S atom of the thiophene. The most obvious possibility is that the Ca atoms abstract sulfur from the thiophene rings to form small clusters of CaS embedded in the polymer, and the two C atoms that lost their bonds to S form new C-C bonds. The simplest C-C bond formation mechanism is ring closure to form a cyclobutadiene ring, but this is probably too unstable. A more energetically favorable reaction would be that the C atoms from two nearby thiophene rings (which both lost their S atoms via abstraction

(41) Thomson, S. W. *Philos. Mag.* **1871**, *42*, 448–452.

**Table 1.** Energies of CaS Clusters (per mole of CaS units) Relative to the Energy of an Isolated (CaS)<sub>1</sub> Molecule, According to DFT Calculations

cluster	$\Delta E$ (kJ/mol)
(CaS) <sub>1</sub>	0
(CaS) <sub>4</sub>	-351
(CaS) <sub>32</sub>	-471
(CaS) <sub>108</sub>	-502
(CaS) <sub>∞</sub>	-503

by Ca) couple, resulting in polymer chain cross-linking. To obtain a crude estimate of the enthalpy of such a reaction, we consider the simplest related reaction for which thermodynamic data are available:



To estimate the heat of this reaction, we use the standard enthalpies of formation of Ca(g) (177.8 kJ/mol), thiophene(l) (80.96 kJ/mol), CaS(s) (-473.21 kJ/mol), and cyclooctatetraene(l) (254.5 kJ/mol).<sup>37</sup> From these values, we obtain a standard reaction enthalpy of -604.7 kJ/mol, which is ~50% larger than the measured heat of 405 kJ/mol in the plateau region below 0.5 ML in Figure 4.

However, depending on their size, the CaS clusters in the polymer are expected to be less stable than bulk CaS(s). To illustrate this size effect, we repeat the calculation of the standard enthalpy of the reaction 1, but use the enthalpy of formation of a single CaS molecule, +123.59 kJ/mol.<sup>42</sup> This time, the reaction enthalpy is only -7.9 kJ/mol compared to -604.7 kJ/mol for the formation of bulk CaS(s). Even if we consider that embedding the CaS molecule in the polymer matrix will make the reaction slightly more exothermic, the difference to the measured heat (-405 kJ/mol) remains very large. This shows that neither single CaS molecules nor bulk CaS can be formed along with cyclooctatetraene, but only small clusters of CaS. To obtain quantitative information about the size dependence of the energy of the CaS clusters, we performed DFT calculations of the cluster stabilization energies  $\Delta E$  relative to the energy of the isolated CaS unit (Table 1; see section 2 for the computational details).

As can be seen, the stabilization energy depends strongly on the cluster size for very small clusters, but approaches rapidly the value for the infinite crystal (CaS)<sub>∞</sub> for clusters larger than (CaS)<sub>108</sub>. Using the values in Table 1, we now relate the difference of 200 kJ/mol between the measured heat (-405 kJ/mol) and the calculated standard reaction enthalpy (-604.7 kJ/mol) to the reduced stability of small CaS clusters relative to bulk CaS. Table 1 shows that the (CaS)<sub>4</sub> cluster is less stable by 152 kJ/mol than bulk (CaS)<sub>∞</sub>, and using interpolation, we estimate that a (CaS)<sub>3</sub> cluster is less stable by 272 kJ/mol than bulk (CaS)<sub>∞</sub>. Therefore, a destabilization of 200 kJ/mol is consistent with the formation of clusters which, on average, contain three to four CaS units. Considering this estimate, we think that the assumed reaction (eq 1) is energetically consistent with our measured heats. There will be additional small energy differences associated with the fact that, in the real Ca/P3HT reaction, the thiophene and cyclooctatetraene units have their C-H bonds partly replaced by C-C bonds to neighboring units. The question arises of whether the CaS molecules are sufficiently mobile in the polymer matrix and on the time scale of

the calorimetry signal (~0.1 s) to diffuse around and form clusters soon enough to have the heat of CaS-CaS bonding show up as part of the heat signal. Since no data for the mobility of CaS in P3HT are available, we will use data for other small molecules in other polymers for a rough estimate. For example, the diffusion coefficient,  $D$ , of CO<sub>2</sub> in poly(ethylene 2,6-naphthalene dicarboxylate) (PEN) is  $4 \times 10^{-14}$  m<sup>2</sup>/s at 293 K.<sup>43</sup> According to the Einstein equation for the mean square displacement,  $\langle x^2 \rangle = 2Dt$ , this corresponds to a mean displacement of ~90 nm within the ~0.1 s time scale of the experiment. Since the mean distance between two neighboring S atoms in P3HT is only ~0.6 nm, the mobility should be more than sufficient for the formation of small clusters, even if CaS is less mobile than CO<sub>2</sub> due to its larger size and dipole moment.

Further support for the formation of CaS comes from a comparison of the observed S 2p XPS shifts (2.8 eV to lower binding energies upon reaction) and the computed core-orbital energy shifts. According to our DFT calculations, the S 2p core orbital energies are shifted to lower binding energies by 2.4–4.1 eV with respect to gas-phase thiophene depending on the size of the CaS clusters considered. Larger clusters are characterized by smaller shifts (2.4–3.7 eV for Ca<sub>32</sub>S<sub>32</sub>, 3.6–3.8 eV for Ca<sub>4</sub>S<sub>4</sub>; final-state effects are not included).

The ~1.5 eV higher Ca 2p binding energy for the “reacted” Ca compared to the 3D Ca(solid) is also consistent with formation of small CaS clusters, if the less efficient screening in the clusters (as compared to the bulk materials) is taken into account.<sup>44–46</sup>

One might expect to notice stronger changes in the C 1s spectra due to the extraction of S from the thiophene ring than the corresponding spectra (Figure 6) show. However, the two C atoms attached to the S atom are of the type -C= within a conjugated  $\pi$  system and would remain so after losing the S neighbor, which in turn is replaced by a C-C nearest neighbor. The two types of C atoms are already present in the pristine polymer (along with aliphatic carbon), and thus, their respective components are part of the C 1s peaks before any reaction with the Ca takes place. Thus, the proposed reaction is compatible with the observed lack of change in the C 1s spectra.

The combined calorimetry, XPS, and LEIS data suggest the following picture of the interaction between Ca and P3HT: Parts of the deposited Ca react with the thiophene units at the surface and in the surface near bulk of the polymer. The reaction involves cleavage of the thiophene ring and formation of calcium sulfide as described above. Concurrently, and especially at higher coverages, 3D Ca islands are formed at the surface of the polymer, until the surface is completely covered with Ca at coverages above 11 ML. Thus, the decrease of the heat of adsorption between 0.6 and 4 ML can be interpreted as a superposition of the reaction (405 kJ/mol) and the formation of Ca clusters (178 kJ/mol, identical to the absolute value of the sublimation enthalpy). [There is also a very high heat, ~600 kJ/mol, at very low Ca coverages (<0.1 ML), which we attribute to reaction with defects or impurities in the polymer and will ignore in the analysis below.]

The simplest approach for interpreting the heat of adsorption curve is a two-site model,<sup>17</sup> which includes sites with higher

(43) Bharadwaj, R. K.; Boyd, R. H. *Polymer* **1999**, *40*, 4229–4236.

(44) Vandoveren, H.; Verhoeven, J. A. T. *J. Electron Spectrosc.* **1980**, *21*, 265–273.

(45) Franzen, H. F.; Merrick, J.; Umana, M.; Khan, A. S.; Peterson, D. T.; McCreary, J. R.; Thorn, R. J. *J. Electron Spectrosc.* **1977**, *11*, 439–443.

(46) Bahadur, S.; Gong, D. L.; Anderegg, J. *Wear* **1996**, *197*, 271–279.

(42) Chase, M. W. J. *J. Phys. Chem. Ref. Data-Monogr.* **1998**, *9*, 1–1951.

adsorption energy (405 kJ/mol, Ca interacting with the polymer S atoms) and other sites with lower adsorption energy (178 kJ/mol, adsorption of Ca onto 3D Ca particles). The step in the dashed line in Figure 4 is placed such that the integral under this curve is identical to the integral under the experimental curve in the range above 0.1 ML. The position of this step indicates that approximately 1.6 ML Ca binds directly to S atoms of the polymer with a heat of 405 kJ/mol, whereas the rest of the Ca binds to Ca islands, releasing the heat of sublimation. The smooth heat curve is interpreted as due to a gradual transition between these two modes of bonding associated with a kinetic competition between Ca diffusing deeper and deeper below the surface to find S atoms and Ca nucleating in clusters on the surface. The former process gets slower as the reacted polymer grows deeper, and the latter gets faster as more and larger Ca clusters are formed.

According to this two-site model, Ca binds exclusively to subsurface S atoms in the coverage range from 0.1 to 0.6 ML, where the Ca heat is nearly constant around 405 kJ/mol in Figure 4. The LEIS results show that only 1–3% of the surface is covered by Ca clusters in this coverage region. Thus, a tiny amount of the Ca is also appearing on the surface already, possibly as Ca clusters, which contribute a lower heat (178 kJ/mol). Correcting the value of 405 kJ/mol for this possible contribution means that the true reaction heat with S may actually be ~6% higher, or up to 430 kJ/mol.

**4.3. Depth Range of Ca Reaction.** In the following, we will make use of the fact that the S 2p XPS measurements at different photon energies probe different depth ranges and thus provide complementary information about the depth up to which the Ca atoms diffuse into and react with the S atoms in the near-surface region of the polymer.

The XPS spectra in Figure 5a were taken at a photon energy of 200 eV, at which the kinetic energy of the S 2p photoelectrons ( $E_{\text{kin}} \approx 34\text{--}41$  eV) is close to their minimum in inelastic mean free path (IMFP),  $\lambda$ . This thus provides high surface sensitivity. Recognizing from the LEIS data that less than 10% of the surface is covered by any 3D Ca particles below 2 ML of adsorbed Ca (Figure 3), it is a good approximation to use only the  $\lambda_{\text{P3HT}}$  value below 2 ML Ca coverage and neglect the faster attenuation through the small amounts of 3D Ca. For the given energy range, we estimate  $\lambda_{\text{P3HT}} = 0.18$  nm on the basis of IMFP data for the structurally very similar poly(3-octylthiophene).<sup>47</sup>

In contrast, the S 2p spectra in Figure 5b where taken with Al K $\alpha$  radiation, 1486.6 eV, which leads to a much larger mean free path of the resulting S 2p photoelectrons [ $\lambda = 4.8$  nm at  $E_{\text{kin}} = 1320$  eV for poly(octylthiophene)].<sup>47</sup> As a result, the signal of “unreacted” sulfur is now visible even at a large Ca coverage of 14 ML.

The thickness of the layer containing exclusively “reacted” sulfur, i.e., the diffusion depth of the Ca atoms, is now calculated by comparing the intensities of the signals for “reacted” and “unreacted” sulfur, relying on the exponential damping of signal intensity at a depth  $z$  below the surface:  $\exp(-z/\lambda)$ .

For our estimation, we adapt an equation introduced by McCafferty and Wightman, who determined the thickness  $d$  of an oxide layer formed on a metal substrate upon oxidation using the relation<sup>48</sup>

$$d = \lambda_{\text{mo}} \sin(\theta) \ln \left[ \left( \frac{D_{\text{m}} \lambda_{\text{mo}}}{D_{\text{mo}} \lambda_{\text{m}}} \right) \left( \frac{I_{\text{mo}}}{I_{\text{m}}} \right) + 1 \right] \quad (2)$$

with  $D$  denoting the atomic density of the probe element (metal there, but sulfur here),  $I$  the intensities,  $\lambda$  the inelastic mean free path of electrons,  $\theta$  the emission angle, and the subscripts m and mo referring to the metal and the metal oxide species, respectively. For the Ca–P3HT system, this simplifies (for  $\theta = 90^\circ$ ) to

$$d = \lambda \ln \left[ \left( \frac{I_{\text{reacted}}}{I_{\text{unreacted}}} \right) + 1 \right] \quad (3)$$

where  $d$  is now the average depth of reacted S in the polythiophene. The concentration of Ca in the polymer is sufficiently low to justify the assumption that  $\lambda \approx \lambda_{\text{P3HT}}$ . Note that this model assumes that there is an abrupt interface between the reacted and unreacted polymer, which is probably not completely true when the reacted depth is large. (However, the rapid decrease of the signal of the unreacted sulfur in the S 2p XPS data taken with 200 eV photons (Figure 5a) and the fact that for coverages exceeding 0.65 ML only the reacted species is visible in the spectra shows that a layer-by-layer reaction of the Ca with the polymer dominates at least for small reaction depths.)

Figure 8a shows plots of this reacted depth of S versus Ca coverage estimated using eq 3 and the reacted:unreacted S 2p intensity ratios from Figures 5 and 7. The data taken at the higher photon energy show that the reacted depth increases with Ca coverage up to ~3 nm. Since the signal of unreacted sulfur at  $h\nu = 200$  eV becomes too small for an accurate estimate at higher coverages, no higher-coverage data are plotted for this experiment. Below 0.5 ML, there is good agreement between the data for both photon energies.

Another, independent estimate of the reaction depth can be derived from the simple two-site interpretation of the heat of adsorption measurements, which show that 1.6 ML of the Ca deposited reacts with the polymer at the highest Ca coverage (see above). This reacted Ca coverage can be converted to a reacted thickness, assuming that each reacted Ca atom binds one sulfur atom of the polymer, by using the mass density (1.33 g/cm<sup>3</sup>)<sup>49</sup> and the stoichiometry of the polymer. This reacted Ca coverage of 1.6 ML ( $= 1.18 \times 10^{15}$  atoms/cm<sup>2</sup>) corresponds to a depth of 2.5 nm at the highest Ca coverage, in excellent agreement with the value of ~3.0 nm obtained from the XPS data in Figure 8a.

To obtain the reacted depths for the lower coverages, we now apply the same type of two-state analysis of the heat data as described above for the highest Ca coverage. Figure 8b shows the results and compares them to the reacted depths derived from XPS. (Note that the integral heat of adsorption minus the heat of sublimation directly gives the amount of Ca in the stronger bonding state at each coverage.) The agreement with the XPS results is remarkably good. Also shown here for comparison is the reacted depth that would result if the adsorbed Ca reacted completely and stoichiometrically with the polymer in a layer-by-layer fashion (dashed line). The good agreement with both data curves at low coverages reveals that the Ca initially, below 1 ML, reacts indeed completely with the

(47) Lesiak, B.; Kosinski, A.; Jablonski, A.; Kover, L.; Toth, J.; Varga, D.; Cserny, I.; Zagorska, M.; Kulszewicz-Bajer, I.; Gergely, G. *Appl. Surf. Sci.* **2001**, *174*, 70–85.

(48) McCafferty, E.; Wightman, J. P. *Surf. Interface Anal.* **1998**, *26*, 549–564.

(49) Cugola, R.; Giovanella, U.; Di Gianvincenzo, P.; Bertini, F.; Catellani, M.; Luzzati, S. *Thin Solid Films* **2006**, *511*, 489–493.



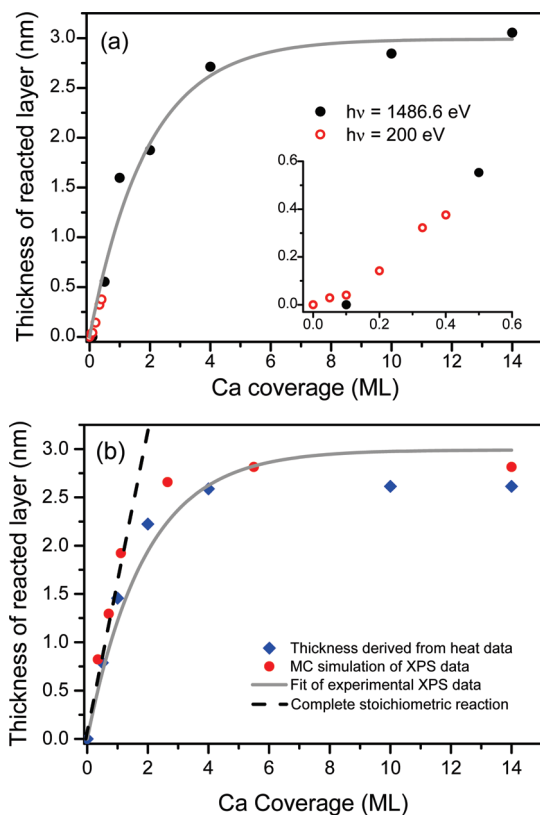


**Figure 8.** (a) Thickness of the reacted layer vs Ca coverage as extracted from the XPS data in Figure 5a (red open circles) and 5b (black closed circles) using eq 3. The gray solid line is an exponential fit with a function of the type  $a(1 - \exp(-bx))$ . The blowup of the low-coverage range (inset) shows good agreement between the two data sets in the low-coverage range. (b) Blue diamond-shaped symbols plot the thickness of the reacted layer determined by analysis of the heat of adsorption data, based on the two-site model and assuming layer-by-layer reaction. This is compared to the results of the XPS data from Figure 8a (gray solid line) and Monte Carlo simulations of the XPS intensities (red closed circles). The dashed line shows the hypothetical reaction depth for the case that all adsorbed Ca reacts stoichiometrically with the polymer in a layer-by-layer fashion. See the text for further details.

polymer. At higher coverages the formation of Ca clusters as the competing process becomes increasingly efficient.

This analysis was verified using the XPS simulation program SESSA by Smekal et al.,<sup>50</sup> which performs Monte Carlo simulations of the electron trajectories based on the partial-intensity approach for the electron-solid interaction.<sup>51</sup> As input parameters, only the stoichiometry and the density ( $1.33 \text{ g/cm}^3$ ) of the material are necessary. Thus, this approach has the very important advantage that no assumptions about the IMFP of the electrons need to be made, as it will be determined as part of the simulation. We used SESSA to simulate the damping of the signal of unreacted P3HT by a layer of reacted P3HT, assuming again an abrupt interface between the two layers. The resulting curve (red open symbols in Figure 8b) shows good agreement with the data derived from the experiment and thus confirms the validity of our approach. (Note that the fraction of the deposited Ca that actually reacts with the polymer is needed to relate the total amount of deposited Ca to the thickness of the reacted layer. This fraction was determined using the calorimetric data as described above.)

In summary, the Ca coverage range over which Ca reacts with sulfur, as revealed by the heats in Figure 4, is very consistent with the range revealed by the XPS data taken at higher photon energy. Note that the LEIS data indicated the existence of a continuous Ca film on top of the polymer for coverages exceeding 11 ML, proving that the coverage of 14 ML indeed represents a Ca excess. We also point out that the damping of S 2p intensities caused by any Ca overlayer does not affect the above thickness calculation, because only the ratio of peak intensities of the two sulfur species was used, which are equally influenced by the Ca layer.

The shape of the Ca sticking probability (S) versus Ca coverage curve (Figure 1) can now be understood. The initial value of 0.4 corresponds to the intrinsic sticking probability of Ca on clean P3HT, which is small because of the very weak attraction of Ca to the dominant  $\text{CH}_2$ , CH, and  $\text{CH}_3$  groups of the polymer. Even if a Ca atom binds to these groups and enters a weakly held mobile precursor state, it may desorb again before it finds a strong binding site and thus would appear as if it did not stick in this measurement. Furthermore, the highly exothermic reaction between Ca and thiophene under formation of CaS involves cleavage of C–S bonds and therefore probably has an activation barrier. This would also lead to a reduced sticking probability. The initial, rapid increase in sticking probability from 0.4 to 0.6 occurs in the first 1/3 ML of Ca, which is approximately the amount of Ca required to react with the sulfur atoms in the first layer of P3HT monomers. Thereafter, the sticking probability slowly increases from 0.6 to 0.7 up to  $\sim 1.4$  ML, when the thiophene groups at the surface have already reacted and additional Ca is mainly reacting with thiophene groups deeper in the polymer. This broad coverage range of nearly constant sticking probability indicates that the intrinsic sticking probability of Ca is  $\sim 0.65 \pm 0.05$  on fully reacted P3HT (i.e., P3HT in which the thiophene units have already reacted with Ca, presumably via a reaction analogous to reaction 1 above). Then, from 1.5 to 2.5 ML, S increases more rapidly again as the growth mode of Ca becomes dominated by the growth of 3D Ca particles on top of the polymer. On the 3D Ca, the sticking probability is clearly higher than on the polymer, with or without subsurface Ca. Eventually, the surface is covered with a continuous overlayer of Ca(s), which has an intrinsic sticking probability of unity, as also observed previously.<sup>17,22</sup>

**4.4. Comparison to Ca Adsorption on Other Polymers.** The qualitative trend of the heat of adsorption versus Ca coverage seen here for Ca on P3HT (Figure 4) is very similar to that previously reported for Ca on poly(methyl methacrylate) (PMMA)<sup>17</sup> and Ca on polyimide (PI)<sup>14</sup> and would probably be even closer if the Ca/PI data had used true measured sticking probabilities instead of assuming unit sticking probability. This suggests that the same basic reaction events are at work in each case. In the present paper, the Ca/P3HT reaction is shown to initially involve a sulfur-specific abstraction mechanism (which requires subsurface diffusion). However, the coverage dependence of the heat requires a kinetic competition between this highly exothermic subsurface reaction and the much less exothermic clustering of Ca on top of the polymer surface to form solid Ca particles and eventually a continuous Ca film. The subsurface reaction dominates initially but, as the diffusion depth required for this reaction increases, it becomes less likely and, as the area covered by Ca clusters increases, Ca addition to these

(50) Smekal, W.; Werner, W. S. M.; Powell, C. J. *Surf. Interface Anal.* **2005**, *37*, 1059–1067.

(51) Werner, W. S. M. *Surf. Interface Anal.* **2005**, *37*, 846–860.

becomes more likely. It must be this same kinetic competition between some highly exothermic reaction below the surface and the clustering of Ca on top of the polymer that is the common feature in the reaction of Ca with these three very different polymers. In the case of PMMA, the highly exothermic subsurface reaction is with ester groups and is also thought to require cleavage of C-heteroatom bonds.<sup>17</sup> In the case of polyimide, the highly exothermic reaction probably involves Ca inducing some subsurface C–O or C–N bond cleavage.

The qualitative trend of the sticking probability for Ca versus Ca coverage seen here for Ca on P3HT (Figure 2) is also very similar to that previously reported for Ca on PMMA.<sup>17</sup> This is also due to the similarity of this kinetic competition. Initially, the sticking probability is low since the polymer surfaces are very inert and the physisorbed Ca atoms must diffuse subsurface to find the dominant reaction sites, during which time the Ca adatom may also desorb. In addition, the initially predominating reaction of Ca with the polymer involves cleavage of C-heteroatom bonds and thus probably has an activation barrier, which reduces the sticking probability, as mentioned above. Once the Ca reacts with the first layer of subsurface thiophenes or esters, this changes the electronic structure of the polymer, which seems to increase its intrinsic sticking probability for Ca. During these stages, the sticking probability is controlled by a kinetic competition between the relative rates of subsurface diffusion and desorption of the very weakly adsorbed Ca atoms. If the Ca-induced change in electronic structure upon reaction of the first layer of subsurface thiophenes or esters is sufficient to increase the former rate or decrease the latter rate, then the sticking probability will increase, as observed. A further increase in sticking probability occurs as Ca particles nucleate and begin to cover a larger and larger fraction of the surface, since Ca sticks with unit probability to Ca surfaces. Unit sticking probability is reached by ~4 ML, well before LEIS shows that the surface is completely covered by Ca (~11 ML). This indicates that Ca traps with nearly unit probability into a weakly bound precursor state on the Ca-free parts of the polymer surface and rapidly diffuses across the surface to find growing Ca clusters. Such behavior is common in metal nucleation and particle growth on surfaces that bind metal atoms only weakly, such as many oxides.<sup>52</sup> This also

explains why the heat of Ca adsorption reaches the bulk heat of sublimation already at 4 ML.

## 5. Conclusions

Calcium adsorbs on poly(3-hexylthiophene) with a high heat of adsorption of 405 kJ/mol between 0.1 and 0.6 ML, which correlates in coverage with the appearance and growth of a new S 2p XPS signal that is shifted by  $-2.8$  eV relative to the respective signal of the unreacted polymer. These findings are attributed to Ca inducing the cleavage of C–S bonds in the thiophene groups below the surface and formation of CaS clusters. LEIS and XPS measurements reveal that Ca ultimately reacts with sulfur atoms down to a depth of ~3 nm, which corresponds to  $1.2 \times 10^{15}$  atoms of reacted sulfur atoms per  $\text{cm}^2$ , or nearly five monomer-unit layers. At high coverage, the adsorbed Ca also forms 3D Ca clusters on the surface of the polymer. This process, which competes with diffusion to the subsurface region and reaction with sulfur, predominates above ~2 ML and leads to the formation of a continuous Ca(solid) multilayer film beyond 11 ML. These competing kinetics can be explained by invoking a transiently adsorbed, mobile Ca species, bound by the very weak attraction of Ca to the dominant polymer moieties ( $\text{CH}_2$ ,  $\text{CH}$ , and  $\text{CH}_3$ ). This adsorbed Ca precursor state can either (1) diffuse to the sulfur atoms of subsurface thiophene units and react, (2) diffuse to find other Ca atoms on the surface and to form Ca clusters, or (3) desorb.

**Acknowledgment.** We thank Prof. G. P. Bartholomew for providing the P3HT sample and Prof. David Ginger for insightful discussions. J.F.Z. thanks the National Natural Science Foundation of China for support through Grant No. 20773111 and the “Hundred Talents Program” of the Chinese Academy of Sciences. F.B. and J.M.G. thank the Deutscher Akademischer Austauschdienst (DAAD) for support through the PPP-USA contracts D/06/29404 and D/08/11868. C.T.C. acknowledges support from the US National Science Foundation under CHE-0757221. J.A.F. would like to acknowledge the Center for Nanotechnology at the UW for an NSF-supported IGERT Award (DGE-0504573). This work was also supported by the Excellence Cluster “Engineering of Advanced Materials” granted to the University of Erlangen-Nürnberg.

**Supporting Information Available:** Reflectivity as a function of Ca coverage and complete ref 24. This material is available free of charge via the Internet at <http://pubs.acs.org>.

JA904844C

(52) Campbell, C. T. *Surf. Sci. Rep.* **1997**, *27*, 1–111.

(53) Zhao, W.; Guo, Y. X.; Feng, X. F.; Zhang, L.; Zhang, W. H.; Zhu, J. F. *Chin. Sci. Bull.* **2009**, *54*, 1978–1982.